


Using a variant of coverslip hypoxia to visualize tumor cell alterations at increasing distances from an oxygen source

Miguel Arocena^{1,2,3}  | Mercedes Landeira^{1,2} | Andrés Di Paolo² | Alejandro Silva⁴ | José Sotelo-Silveira^{1,2} | Ariel Fernández⁴ | Julia Alonso⁴

¹Sección Biología Celular, Facultad de Ciencias, Universidad de la República, Montevideo, Uruguay

²Departamento de Genómica, Instituto de Investigaciones Biológicas Clemente Estable, Montevideo, Uruguay

³Cátedra de Bioquímica y Biofísica, Facultad de Odontología, Universidad de la República, Montevideo, Uruguay

⁴Instituto de Física, Facultad de Ingeniería, Universidad de la República, Montevideo, Uruguay

Correspondence

Miguel Arocena, Cátedra de Bioquímica y Biofísica, Facultad de Odontología, Universidad de la República, Las Heras 1925, Montevideo 11600, Uruguay.
Email: m.arocena.sutz@gmail.com

Funding information

Comisión Sectorial de Investigación Científica (CSIC), Grant/Award Number: 331; Programa de Desarrollo de las Ciencias Básicas (PEDECIBA); Agencia Nacional de Investigación e Innovación (ANII)

Abstract

Early stages in tumor development involve growth in confined spaces, where oxygen diffusion is limited and metabolic waste products accumulate. This hostile microenvironment imposes strong selective pressures on tumor cells, leading eventually to the survival and expansion of aggressive subclones that condition further tumor evolution. To model features of this microenvironment in vitro, a diffusional barrier can be introduced in the form of a coverslip placed on top of cells, a method termed coverslip hypoxia. Using a variant of this method, with larger volume between coverslip and cells and with oxygen diffusion occurring only through a small hole in the center of the coverslip, we have visualized alterations in LNCaP tumor cells as a function of their distance to the oxygen source at the center. We observed remarkable morphological changes in LNCaP cells as the distance from the center increases, with cells becoming highly spread, displaying dynamic membrane protrusions and occasionally adopting a migratory phenotype. Concomitantly, cells farther from the center displayed marked increases in the hypoxia marker hypoxyprobe, whereas extracellular pH decreased in the same direction. Cells with altered morphology displayed prominent increases in fibrillar actin, as well as swollen mitochondria with distorted cristae and accumulation of neutral lipid-containing intracellular vesicles. These results show that an in vitro microenvironment that models diffusional barriers encountered by tumors in situ can have profound effects on tumor cells. The coverslip hypoxia variant we describe can be used to characterize in vitro the response of tumor cells to environmental conditions that play crucial roles in early tumor development.

KEYWORDS

coverslip hypoxia, hypoxia gradient, in vitro tumor microenvironment

1 | INTRODUCTION

The tumor microenvironment is markedly distinct from normal tissue microenvironments. In epithelia, initial tumor growth is limited by the basal lamina, which prevents access to the underlying stroma, where blood vessels serve as the source of oxygen and nutrients (Gatenby & Gillies, 2004). Oxygen diffusion in the extracellular medium is limited, with an estimated 200 μm as the distance between a cell and the nearest

capillary at which hypoxia ensues (Olive, Vikse, & Trotter, 1992). As a consequence, central regions in early tumor masses distant from the vasculature develop hypoxia and also acidosis, as cells switch from oxidative phosphorylation to glycolysis (Gillies & Gatenby, 2007; Helmlinger, Sckell, Dellian, Forbes, & Jain, 2002). Hypoxia and acidification impose strong selective forces on tumor evolution, favoring the emergence of tumor subclones with more invasive phenotypes (Gillies & Gatenby, 2007; Gillies, Raghunand, Karczmar, & Bhujwala, 2002; Lloyd

et al., 2016). In vitro, regional variations in oxygen availability and extracellular pH mimicking the early tumor microenvironment can be reproduced in three-dimensional culture systems, such as tumor spheroids, which beyond a certain size develop hypoxia and acidification in their central regions (Alvarez-Pérez, Ballesteros, & Cerdán, 2005; Laurent et al., 2013). However, despite the development of new techniques, such as light sheet fluorescent microscopy, visualizing noninvasively the deep regions within tumor spheroids remains challenging (Pampaloni, Ansari, & Stelzer, 2013). An alternative approach is to place a coverslip on top of a cell monolayer, so that oxygen can only diffuse through the narrow space between the cells and the edges of the coverslip, a method termed coverslip hypoxia (Pitts & Toombs, 2004). Using this method in combination with oxygen-sensitive green fluorescent protein (GFP) fluorescence shifts, it was shown that oxygen levels in cells under coverslips decreased from the edges toward the center of the coverslip (Takahashi & Sato, 2010). In this study, we have used a variant of coverslip hypoxia to visualize the response of tumor cells to changes in their microenvironment similar to those encountered during early tumor development. To minimize effects because of reduced medium volume (Pitts & Toombs, 2004), we increased the volume between the cells and the coverslip on top, and we also changed the location of the oxygen source to a small hole in the center of the coverslip, so that oxygen availability would be reduced toward regions at the periphery of the coverslip. Using the LNCaP prostate cancer cell line, we have observed a strong increase in the hypoxia marker hypoxyprobe (Laurent et al., 2013; P. Liu et al., 2014) as the distance toward the center of the coverslip increases, accompanied by concomitant extracellular pH decreases and by dramatic morphological, ultrastructural, and dynamic changes. Our results further support the use of the coverslip hypoxia method as a simple but revealing approach to model the oxygen diffusion restriction of the early tumor microenvironment and its effects on the tumor cell phenotype.

2 | MATERIALS AND METHODS

2.1 | Coverslip hypoxia variant

Instead of placing a coverslip directly on the top of a cell monolayer, we cultured cells in the wells of 35-mm glass bottom dishes (Cellvis, Mountain View, CA) and covered the wells with coverslips. The wells were 20 mm in diameter and 1 mm in depth. We used custom square acrylic coverslips, 24 mm in width and 2 mm in thickness, with a 1-mm wide square hole in the middle made with a laser cutter. As the well diameter is smaller than the coverslip, the well becomes sealed at its outer edge when the coverslip is slightly pressed against the floor of the glass bottom dish, leaving the square hole in the middle of the coverslip as the only expected source of oxygen. The coverslip hypoxia variant is schematically depicted in Figure 1a.

2.2 | Cell culture and coverslip hypoxia treatment

LNCaP prostate cancer cells (ATCC, Manassas, VA) were maintained in (Roswell Park Memorial Institute) RPMI 1640 supplemented

with 10% fetal bovine serum and penicillin/streptomycin. A total of 10^5 cells were plated in the well of a 35-mm glass bottom dish, allowed to attach for 24 hr, then the well was covered with a coverslip and after another 24 hr cells were observed.

2.3 | Cell staining, extracellular pH visualization, and confocal microscopy

For fixed cell staining, cells were fixed 10 min with 4% paraformaldehyde, washed in phosphate-buffered saline, permeabilized with 0.1% Triton X-100, and stained for 30 min with Alexa Fluor 488 phalloidin or for 15 min with Nile red (both from Invitrogen, Waltham, MA). To visualize mitochondria, live cells were stained with the mitochondrial probe Mitotracker (Invitrogen), at a final concentration of 200 nM in the medium. For hypoxia staining, we used a hypoxia detection kit (Hypoxyprobe, Burlington, MA), in which cells under coverslips were incubated with the hypoxia marker pimonidazole for 2 hr at a final concentration of 200 μ M in the medium. Next, cells were fixed and permeabilized as before, blocked with 3% bovine serum albumin, and stained with an antibody that recognizes pimonidazole adducts conjugated to DylightTM 549 fluorophore. Nuclei were stained with 4',6-diamidino-2-phenylindole (Invitrogen). We visualized changes in extracellular pH by adding to the medium the pH-sensitive fluorescent dye bis-carboxyethylcarboxy-fluorescein-free acid (BCECF-free acid; Biotium, Fremont, CA), at a final concentration of 5 μ M. Cells were visualized with a Zeiss LSM 800 confocal microscope.

2.4 | Time-lapse imaging

Time-lapse images of migrating LNCaP cells were acquired at 5 min intervals by phase-contrast microscopy, using a $\times 10$ objective and a Nikon Diaphot inverted microscope. Time-lapse images of dynamic protrusions were acquired at 2.5–5 s intervals by differential interference contrast microscopy (DIC), using a $\times 40$ objective and a Zeiss LSM 800 confocal microscope.

2.5 | Transmission electron microscopy

Cells were seeded in the Aclar film inside 35-mm culture dishes, and after the coverslip treatment, they were fixed by adding glutaraldehyde to the cell medium at 2.5% final concentration, for 30 min at 37°C. Cells were further processed for flat embedding and ultramicrotomy, as described previously (Jiménez-Riani et al., 2017), and ultrathin sections were observed with a Jeol JEM1010 transmission electron microscope.

3 | RESULTS

3.1 | Effect of a coverslip hypoxia variant on LNCaP cell morphology, hypoxic state, and extracellular pH

We modified previous versions of the coverslip hypoxia method by culturing cells in the wells of 35-mm glass bottom dishes and sealing the

wells with coverslips larger than the diameter of the well. The coverslips have a small hole in the center, and therefore cells inside the well at increasing distances from the center are expected to become progressively more hypoxic (Figure 1a). When we cultured the LNCaP cells inside the wells and placed a coverslip for 24 hr, we observed marked morphological changes as the location of the cells moved farther away from the center (Figure 1b). Cells became markedly more flattened, often with abundant protrusions, compared with the rounded cell shape observed in control cells and in many cells close to the center of the well. Next, we used the hypoxia marker pimonidazole, which forms adducts predominantly with thiol-containing proteins in conditions of $pO_2 < 10$ mmHg, which can then be detected by immunofluorescence (Raleigh, Chou, Arteel, & Horsman, 1999). After 24 hr of coverslip treatment, we detected a strong gradient of fluorescence intensity, increasing markedly toward the periphery of the well (Figure 2). Therefore, this modified coverslip hypoxia method can be used to induce increasing levels of hypoxia as cells move farther away from an oxygen source. Next, we asked whether these increased levels of hypoxia would translate into a more acidic extracellular pH, presumably by shifting cell metabolism toward anaerobic glycolysis (Helmlinger et al., 2002). We used the pH-sensitive, cell-impermeant probe BCECF-free acid, which decreases its fluorescence emission intensity with decreasing pH (Athmann et al., 2000). Again, after 24 hr

of coverslip treatment, we observed a center to periphery gradient, with BCECF-free acid fluorescence intensity decreasing markedly at the periphery (Figure 3), indicating that extracellular pH becomes more acidic in the region where cells display stronger hypoxia signals.

Taken together, our results show that this simple coverslip hypoxia variant, applied to LNCaP cells, can be used to create a microenvironment where cells become more hypoxic and extracellular pH decreases as the distance from an oxygen source increases.

3.2 | Alterations in LNCaP cells ultrastructure induced by the coverslip hypoxia variant

The morphological change we observed in LNCaP cells after coverslip treatment was accompanied by a marked increase in fibrillar actin staining, with actin fibers often extending throughout the whole cytoplasm, a pattern not seen in cells close to the oxygen source (Figure 4a). Hypoxia has been shown to cause alterations in mitochondrial morphology and to increase the accumulation of lipid droplets containing neutral lipids (X. Liu & Hajnóczky, 2011; Mylonis et al., 2012). After coverslip treatment, LNCaP cells in the periphery of wells showed remarkably rounded and swollen mitochondria, as seen by staining with the mitochondrial probe Mitotracker (Figure 4b). Also,

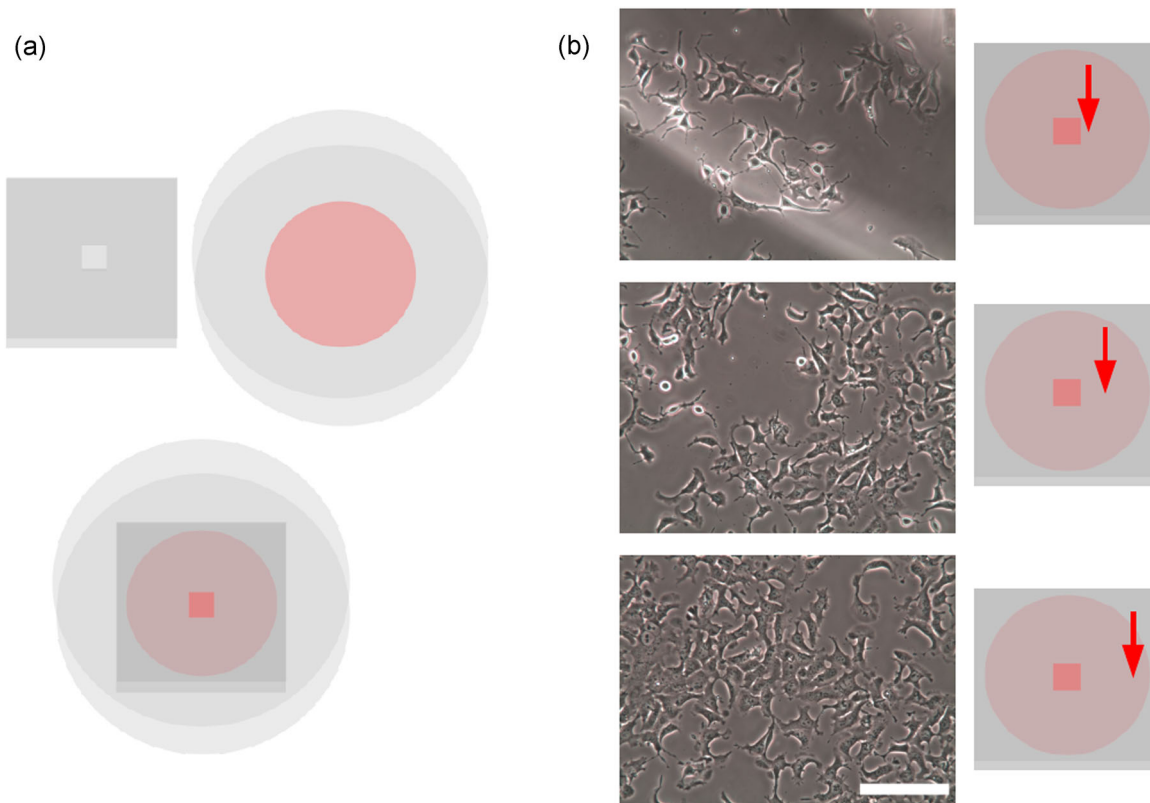
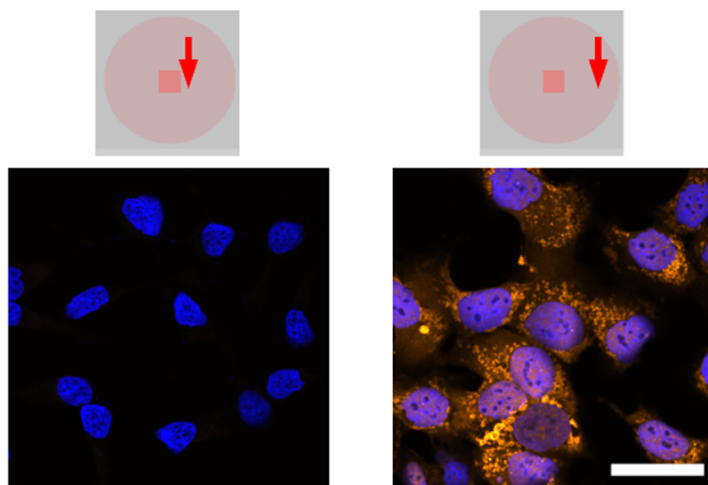


FIGURE 1 A variant of the coverslip hypoxia method. (a) Schematic of the method used, in which a thick coverslip with a small square hole in the middle completely covers the cell containing well of a 35mm glass bottom dish, sealing the outer edge of the well. The hole in the middle of the coverslip is expected to be the only source of oxygen for cells. (b) Morphological change of LNCaP cells as their distance to the oxygen source increases. Scale bar = 50 μ m [Color figure can be viewed at wileyonlinelibrary.com]

(a)



(b)

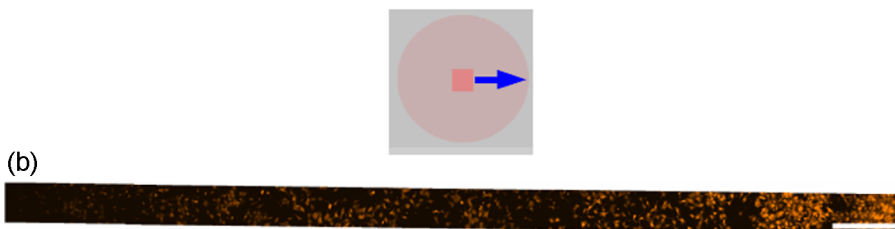


FIGURE 2 Gradient of the hypoxia marker pimonidazole. (a) Pimonidazole adduct staining (orange), in the center and the periphery of the well (DAPI staining of nuclei shown in blue). Scale bar = 20 μm . (b) A stitched image showing pimonidazole adduct staining from the center of the well to the periphery. Scale bar = 500 μm . DAPI: 4',6-diamidino-2-phenylindole [Color figure can be viewed at wileyonlinelibrary.com]

LNCaP cells in the periphery showed marked accumulation of neutral lipid-containing droplets (Figure 4c), detected by Nile red staining using excitation and emission at 510/582 nm, corresponding to the interaction of this dye with neutral lipids (Greenspan & Fowler, 1985). These results were confirmed by transmission electron microscopy, showing that cells in the periphery of wells with coverslips had swollen mitochondria, often with remarkably convoluted cristae and an electron-dense intermembrane space, and also displayed abundant lipid droplets (Figure 5). Therefore, as the distance from the oxygen source increases, cells undergo marked ultrastructural changes consistent with a hypoxic phenotype.

3.3 | Changes in protrusion dynamics and cell migration induced by the coverslip hypoxia variant

The remarkable change in cell shape shown by LNCaP cells after coverslip treatment suggested that in this condition, dynamic behaviors such as extension and retraction of protrusions and cell migration might be increased. LNCaP cells under normoxic conditions displayed relatively quiescent protrusions and very limited motility, whereas cells after coverslip treatment showed more dynamic protrusions, including examples of membrane ruffling, and even formation of lamellipodia and active cell

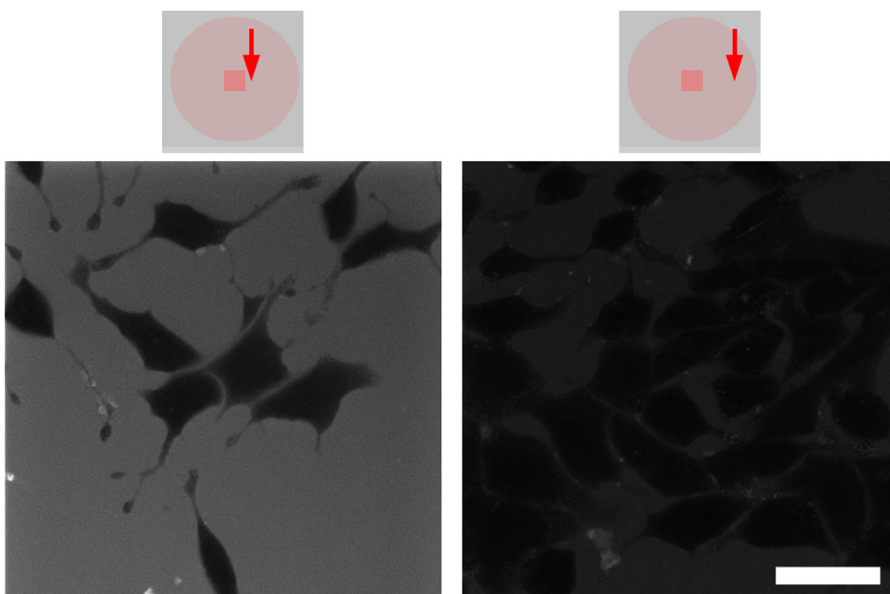


FIGURE 3 Decrease in extracellular pH as the distance from the oxygen source increases. Representative images from the same well show fluorescence of the cell-impermeant BCECF-free acid, which decreases markedly at the periphery of the well. Scale bar = 20 μm . BCECF: bis-carboxyethylcarboxy-fluorescein [Color figure can be viewed at wileyonlinelibrary.com]

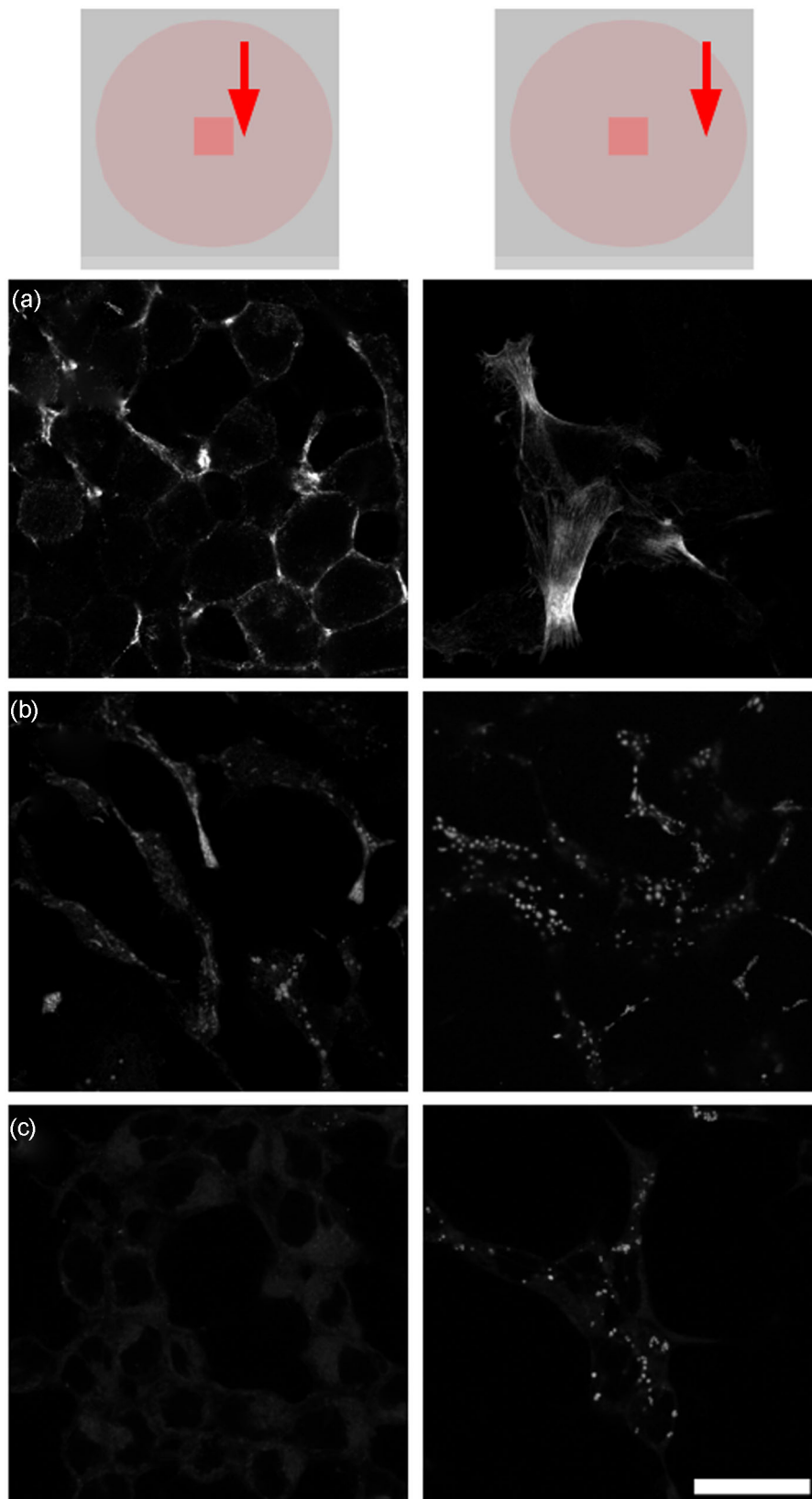


FIGURE 4 Cytoplasmic alterations of LNCaP cells as the distance from the oxygen source increases. (a) Actin staining. (b) Mitochondrial staining. (c) Nile red staining of neutral lipid droplets. Scale bar = 20 μm [Color figure can be viewed at wileyonlinelibrary.com]

migration (Figure 6; Videos S1–S3). Therefore, the microenvironment generated by the coverslip hypoxia variant provides cues that stimulate an increase in the dynamic behavior of LNCaP cells.

4 | DISCUSSION

In the present study, we have modified the coverslip hypoxia method, and we have shown that in combination with the use of LNCaP cells,

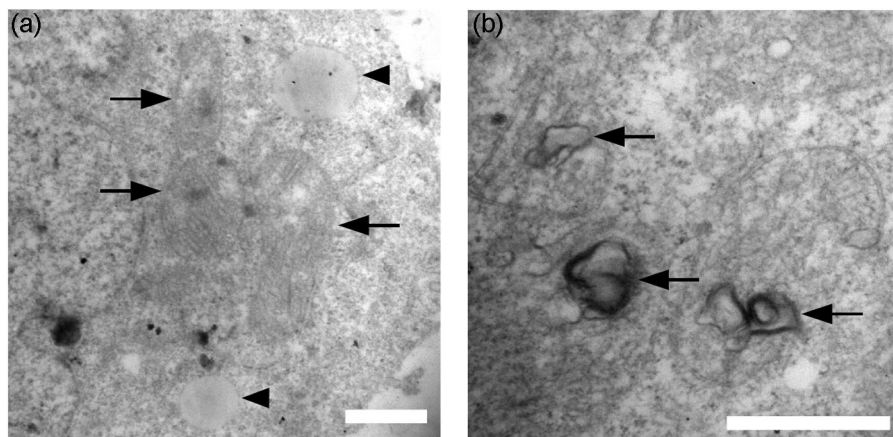


FIGURE 5 Ultrastructure of LNCaP cells at the periphery of wells with coverslips. (a) Lipid droplets (arrowheads) close to mitochondria (arrows). (b) Convoluted mitochondrial cristae and electron-dense intermembrane space (arrows). Scale bar = 1 μm

our variant of this method generates a microenvironment where cells become more hypoxic, extracellular pH becomes more acidic, and cell morphology becomes increasingly altered as the distance from the oxygen source increases. Moreover, cells in more hypoxic regions show distorted mitochondrial morphology and lipid droplet

accumulation, which are ultrastructural alterations associated with hypoxia, and also increases in protrusive activity, and, in some cases, in migratory activity as well.

After 24 hr of coverslip treatment, LNCaP prostate cancer cells become markedly positive for pimonidazole staining at increasing

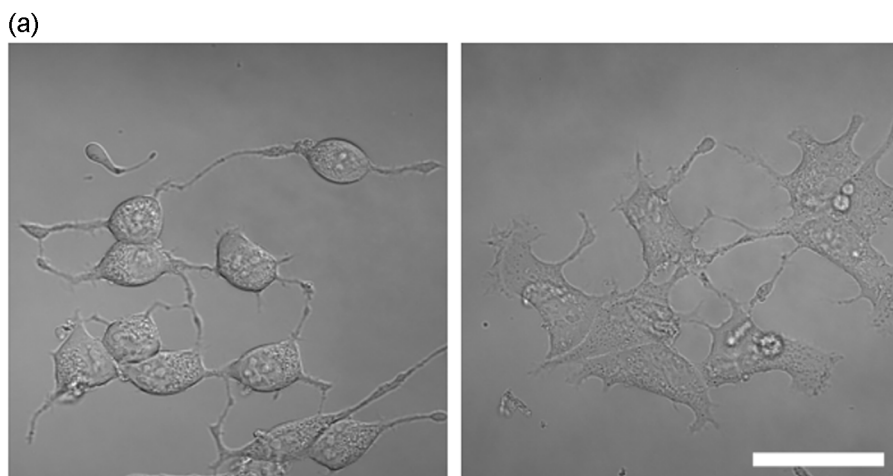


FIGURE 6 Dynamic behavior of LNCaP cells. (a) DIC images of LNCaP cells under normoxic conditions (left) and in the periphery of wells covered with coverslips (right), showing distinct types of protrusions (see also Videos S1 and S2). Scale bar = 20 μm . (b) Composite of phase-contrast images of a migrating LNCaP cell at the periphery of a well covered with a coverslip, showing a polarized, migratory morphology, and active cell motility (see also Video S3). Scale bar = 10 μm . DIC: differential interference contrast microscopy [Color figure can be viewed at wileyonlinelibrary.com]

distance from the oxygen source at the center of the coverslip. In patients with prostate cancer that received pimonidazole before prostatectomy, it was found that strong pimonidazole adduct staining was associated with higher clinical stage and with lymph node metastasis (Ragnum et al., 2015). Moreover, in that study, pimonidazole-positive tumors showed increased expression of hypoxia-related genes. Among them was hypoxia-inducible lipid-droplet-associated, also known as HIG2, and recent results have shown that this gene plays key roles in promoting the formation of lipid droplets in hypoxia and in inhibiting fatty acid oxidation in hypoxic cells, a metabolic shift that is crucial for their survival (Zhang et al., 2017). Our results, showing high pimonidazole adduct staining and lipid droplet formation in LNCaP prostate cancer cells after coverslip hypoxia, are therefore consistent with in vivo results of prostate cancer biopsies that also show high pimonidazole staining and induction of genes essential for lipid droplet formation.

Hypoxia has been shown to stimulate cell motility, and, in particular, it can promote the dissemination of individual cells and metastatic spread (Lehmann et al., 2017). In tumor xenografts, it has been observed that areas with high pimonidazole adduct staining are the source of cells that subsequently migrate toward blood vessels, leading to both local recurrence and eventual metastatic dissemination (Harada et al., 2012). These in vivo results are also consistent with the induction of the protrusive activity and the cell motility that we have observed in our coverslip hypoxia variant.

A lowered extracellular pH is an important component of the tumor microenvironment, and several lines of evidence suggest that it is related to metastatic potential (Kato et al., 2013). Our coverslip hypoxia variant, showing lowered extracellular pH in regions corresponds to higher pimonidazole adduct staining, recapitulates therefore another important feature of the tumor microenvironment and has the potential to contribute to the study of how hypoxia and lowered extracellular pH, among other factors, combine to promote tumor aggressiveness.

In conclusion, we have shown that a variant of the coverslip hypoxia method can create a progressively more hypoxic and acidified microenvironment as the distance from an oxygen source increases and that LNCaP prostate cancer cells in this microenvironment not only become hypoxic but also undergo remarkable morphological, ultrastructural, and dynamic transformations. This coverslip hypoxia variant can, therefore, be a useful method to model critical features of the tumor microenvironment and to study the links between tumor microenvironment and tumor development and evolution.

ACKNOWLEDGMENTS

This work was supported by Comisión Sectorial de Investigación Científica (CSIC) (Grant number ID 331), Programa de Desarrollo de las Ciencias Básicas (PEDECIBA), and Agencia Nacional de Investigación e Innovación (ANII). We acknowledge the Electron Microscopy Service of Facultad de Ciencias, UDELAR.

CONFLICT OF INTERESTS

The authors declare that they have no conflict of interests.

AUTHOR CONTRIBUTIONS

M. A. conceived the study. M. A. and M. L. designed and performed experiments and analyzed data. A. D. P. assisted with imaging. A. S., J. S.-S., A. F., and J. A. assisted with experimental design and data analysis. M. A. wrote the paper. All authors read and approved the final manuscript.

REFERENCES

- Alvarez-Pérez, J., Ballesteros, P., & Cerdán, S. (2005). Microscopic images of intraspheroidal pH by ¹H magnetic resonance chemical shift imaging of pH sensitive indicators. *Magnetic Resonance Materials in Physics, Biology and Medicine*, 18(6), 293–301.
- Athmann, C., Zeng, N., Kang, T., Marcus, E. A., Scott, D. R., Rektorschek, M., & Sachs, G. (2000). Local pH elevation mediated by the intrabacterial urease of *Helicobacter pylori* cocultured with gastric cells. *The Journal of Clinical Investigation*, 106(3), 339–347.
- Gatenby, R. A., & Gillies, R. J. (2004). Why do cancers have high aerobic glycolysis? *Nature Reviews Cancer*, 4(11), 891–899.
- Gillies, R. J., & Gatenby, R. A. (2007). Hypoxia and adaptive landscapes in the evolution of carcinogenesis. *Cancer and Metastasis Reviews*, 26(2), 311–317.
- Gillies, R. J., Raghunand, N., Karczmar, G. S., & Bhujwalla, Z. M. (2002). MRI of the tumor microenvironment. *Journal of Magnetic Resonance Imaging*, 16(4), 430–450.
- Greenspan, P., & Fowler, S. D. (1985). Spectrofluorometric studies of the lipid probe, Nile red. *Journal of Lipid Research*, 26(7), 781–789.
- Harada, H., Inoue, M., Itasaka, S., Hirota, K., Morinibu, A., Shinomiya, K., & Hiraoka, M. (2012). Cancer cells that survive radiation therapy acquire HIF-1 activity and translocate towards tumour blood vessels. *Nature Communications*, 3(1), 783.
- Helmlinger, G., Sckell, A., Dellian, M., Forbes, N. S., & Jain, R. K. (2002). Acid production in glycolysis-impaired tumors provides new insights into tumor metabolism. *Clinical Cancer Research*, 8(4), 1284–1291.
- Jiménez-Riani, M., Díaz-Amarilla, P., Isasi, E., Casanova, G., Barbeito, L., & Olivera-Bravo, S. (2017). Ultrastructural features of aberrant glial cells isolated from the spinal cord of paralytic rats expressing the amyotrophic lateral sclerosis-linked SOD1G93A mutation. *Cell and Tissue Research*, 370(3), 391–401.
- Kato, Y., Ozawa, S., Miyamoto, C., Maehata, Y., Suzuki, A., Maeda, T., & Baba, Y. (2013). Acidic extracellular microenvironment and cancer. *Cancer Cell International*, 13(1), 89.
- Laurent, J., Frongia, C., Cazales, M., Mondesert, O., Ducommun, B., & Lobjois, V. (2013). Multicellular tumor spheroid models to explore cell cycle checkpoints in 3D. *BMC Cancer*, 13(1), 73.
- Lehmann, S., te Boekhorst, V., Odenthal, J., Bianchi, R., van Helvert, S., Ikenberg, K., & Friedl, P. (2017). Hypoxia induces a HIF-1-dependent transition from collective-to-amoeboid dissemination in epithelial cancer cells. *Current Biology*, 27(3), 392–400.
- Liu, P., Wang, Z., Brown, S., Kannappan, V., Tawari, P. E., Jiang, W., & Wang, W. (2014). Liposome encapsulated disulfiram inhibits NFκB pathway and targets breast cancer stem cells in vitro and in vivo. *Oncotarget*, 5(17), 7471–7485.
- Liu, X., & Hajnóczky, G. (2011). Altered fusion dynamics underlie unique morphological changes in mitochondria during hypoxia-reoxygenation stress. *Cell Death & Differentiation*, 18(10), 1561–1572.
- Lloyd, M. C., Cunningham, J. J., Bui, M. M., Gillies, R. J., Brown, J. S., & Gatenby, R. A. (2016). Darwinian dynamics of intratumoral

- heterogeneity: Not solely random mutations but also variable environmental selection forces. *Cancer Research*, 76(11), 3136–3144.
- Mylonis, I., Sembongi, H., Befani, C., Liakos, P., Siniosoglou, S., & Simos, G. (2012). Hypoxia causes triglyceride accumulation by HIF-1-mediated stimulation of lipin 1 expression. *Journal of Cell Science*, 125(14), 3485–3493.
- Olive, P. L., Vikse, C., & Trotter, M. J. (1992). Measurement of oxygen diffusion distance in tumor cubes using a fluorescent hypoxia probe. *International Journal of Radiation Oncology, Biology, Physics*, 22(3), 397–402.
- Pampaloni, F., Ansari, N., & Stelzer, E. H. K. (2013). High-resolution deep imaging of live cellular spheroids with light-sheet-based fluorescence microscopy. *Cell and Tissue Research*, 352(1), 161–177.
- Pitts, K. R., & Toombs, C. F. (2004). Coverslip hypoxia: A novel method for studying cardiac myocyte hypoxia and ischemia in vitro. *American Journal of Physiology. Heart and Circulatory Physiology*, 287(4), H1801–H1812.
- Ragnum, H. B., Vlatkovic, L., Lie, A. K., Axcrona, K., Julin, C. H., Frikstad, K. M., & Lyng, H. (2015). The tumour hypoxia marker pimonidazole reflects a transcriptional programme associated with aggressive prostate cancer. *British Journal of Cancer*, 112(2), 382–390.
- Raleigh, J. A., Chou, S. -C., Arteel, G. E., & Horsman, M. R. (1999). Comparisons among pimonidazole binding, oxygen electrode measurements, and radiation response in C3H mouse tumors. *Radiation Research*, 151(5), 580.
- Takahashi, E., & Sato, M. (2010). Imaging of oxygen gradients in monolayer cultured cells using green fluorescent protein. *American Journal of Physiology. Cell Physiology*, 299(6), C1318–C1323.
- Zhang, X., Saarinen, A. M., Hitosugi, T., Wang, Z., Wang, L., Ho, T. H., & Liu, J. (2017). Inhibition of intracellular lipolysis promotes human cancer cell adaptation to hypoxia. *eLife*, 6, 6. <https://doi.org/10.7554/eLife.31132>

SUPPORTING INFORMATION

Additional supporting information may be found online in the Supporting Information section at the end of the article.

How to cite this article: Arocena M, Landeira M, Di Paolo A, et al. Using a variant of coverslip hypoxia to visualize tumor cell alterations at increasing distances from an oxygen source. *J Cell Physiol*. 2019;234:16671–16678. <https://doi.org/10.1002/jcp.28507>